Active Vibration Suppression of a Smart Beam by Using an LQG Control Algorithm

Cem Onat[1] , Melin Sahin[2], Yavuz Yaman[3,*]

[1] Department of Aerospace Engineering, Middle East Technical University, Ankara, Turkey
Department of Mechanical Engineering, Inonu University, Malatya, Turkey
conat@inonu.edu.tr

[2] Department of Aerospace Engineering, Middle East Technical University, Ankara, Turkey
msahin@metu.edu.tr

[3] Department of Aerospace Engineering, Middle East Technical University, Ankara, Turkey
yyaman@metu.edu.tr

ABSTRACT

The aim of this study was to design and experimentally apply a Linear Quadratic Gaussian (LQG) controller for the active vibration suppression of a smart beam. The smart beam was a cantilever aluminum beam with eight symmetrically located surface-bonded PZT (Lead-Zirconate-Titanate) patches which were utilized both as sensor or actuator depending on their location. A group of PZT patches closed to the root of the beam was used as actuators in the bimorph configuration and a single patch was nominated as a sensor. LQG controller, which is the result of a modern state-space technique, was used in order to design a dynamic optimal regulator. The controller was expected to provide a trade-off between the regulation performance and control effort and it also took process disturbance and measurement noise into consideration. The LQG regulators of the current study were evaluated via closed loop frequency domain simulations in order to regulate the vibration level of the smart beam around zero value. For the experimental verifications, a harmonious controller was selected based on the performed trade-offs between the performance and measurement noise rejection levels. The experimentally obtained time domain responses have demonstrated that the designed controller successfully suppressed the vibration levels of the first flexural mode of the smart beam.

Keywords: *smart beam, PZT, vibration, LQG control*

1 Introduction

The smart structure is a structure that can sense external disturbance and respond to that in real time to fulfill operational requirements. Smart structures consist of a passive structure, highly distributed active devices called smart materials/elements and processor networks [1]. The smart materials/elements are primarily used as sensors and/or actuators and are either embedded in or surface bonded to the existing passive structure [2-4].

The transformation of electrical signal to mechanical deformation enables piezoelectric materials to be used as actuators. Additionally the mechanical deformation of the piezoelectric material can be detected by its electrical response, hence provides the piezoelectric materials to be utilized as sensors as well. Nowadays, a widespread application area of piezoelectric materials is, using them as collocated actuator and sensor pair for active vibration control purposes [5].

In this study, a least order possible LQG controller was designed for the vibration suppression of a smart beam, by using the PZT (Lead-Zirconate-Titanate) patches as sensor and actuator pairs. Various control cases were developed and applied.

* Corresponding author

2 Smart Beam

The smart beam given in Figure 1.a is a cantilever aluminium beam having the dimensions of 490 x 51 x 2 mm and with eight surface bonded SensorTech - BM500 (25 x 20 x 0.5 mm) PZT (Lead - Zirconate -Titanate) patches. A typical patch is shown in Figure 1.b. [6]. A thin isolation layer is placed between the aluminium beam and PZT patches, so that each PZT patch may be employed as a sensor and an actuator independently.

(a) (b)

Figure 1: (a) Smart beam (b) Piezoelectric patch (SensorTech - BM500 PZT Patch)

In this study, piezoelectric patches are labeled according to their positions on each surface of the aluminium beam. As shown in Figure 2, on surface A, piezoelectric patches are labeled from 1 to 4 in clockwise direction and on surface B, they are labeled from 1 to 4 in counter-clockwise direction. Piezoelectric patches are identified by number and surface names, such as piezoelectric patch 1A.

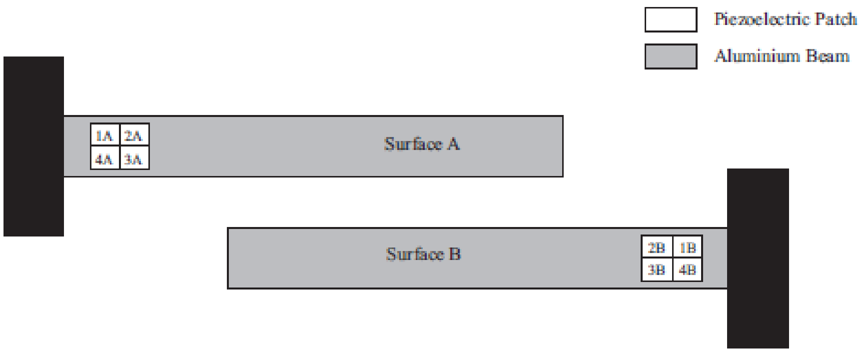

Figure 2: Piezoelectric patches on the smart beam

3 Experimental System Identification

Piezoelectric patches of the smart beam were used as actuators and sensors to obtain the necessary experimental frequency response of the smart beam for system identification. For this purpose, the smart beam was excited with the piezoelectric actuator patches (1A-1B and 4A-4B) and the response of the smart beam was obtained from the piezoelectric sensor patch (2A).

Figure 3 shows experimental setup used for the determination of the experimental frequency response of the smart beam. The excitation signal was a swept sine signal from 2 Hz to 18 Hz with 5 V peak-to-peak value generated by HP33120A signal generator. This generated signal was amplified 30 times by SensorTech SA10 High Voltage Amplifier which also uses SensorTech SA21 High Voltage Power Supply. The amplified excitation signal was then fed to piezoelectric actuator patches. Brüel and Kjær PULSE 3560C platform was used for the determination of the frequency response.

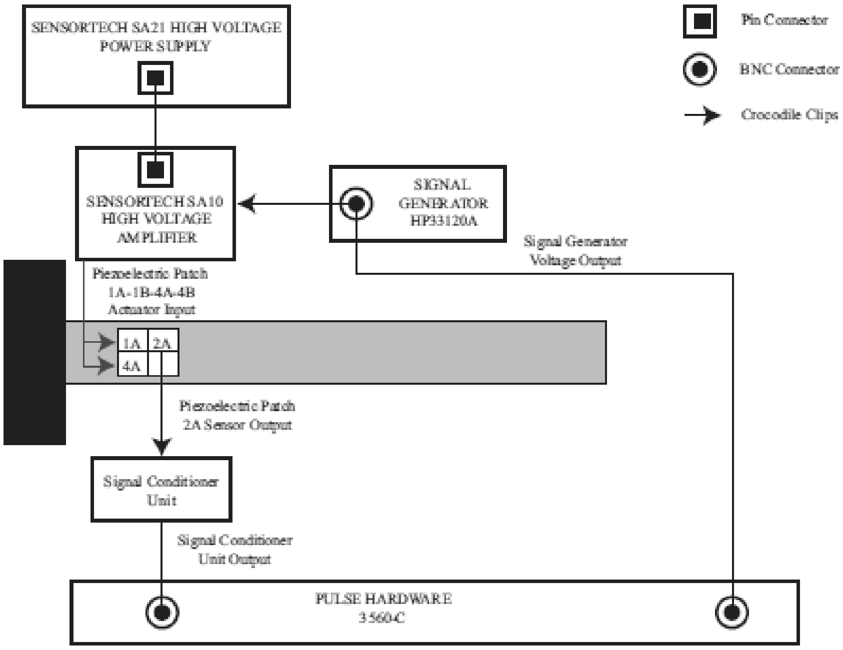

Figure 3: Experimental setup for system identification

The mathematical model of the smart beam was obtained by processing the measured frequency response data. By using MATLAB's "fitsys" command located in μ Analysis and Synthesis Toolbox [7], the transfer function of the smart beam was determined. MATLAB "fitsys" command builds a state-space model based on estimated transfer function. Transfer function of the smart beam is estimated within the frequency range between 2 Hz and 18 Hz. This frequency range includes first flexural mode of the smart beam. Hence a transfer function of the smart beam, being a 6th order one, was obtained and is given in Equation 1.

$$G(s) = \frac{0.06449 \cdot s^6 + 13.42 \cdot s^5 + 288.7 \cdot s^4 + 54660 \cdot s^3 + 3.548 \cdot 10^5 \cdot s^2 + 5.55 \cdot 10^7 \cdot s + 7.102 \cdot 10^7}{s^6 + 191.6 \cdot s^5 + 6085 \cdot s^4 + 741800 \cdot s^3 + 1.211 \cdot 10^7 \cdot s^2 + 7.179 \cdot 10^8 \cdot s + 7.89 \cdot 10^9} \tag{1}$$

Figure 4 shows the experimentally measured and analytically estimated transfer functions of the smart beam.

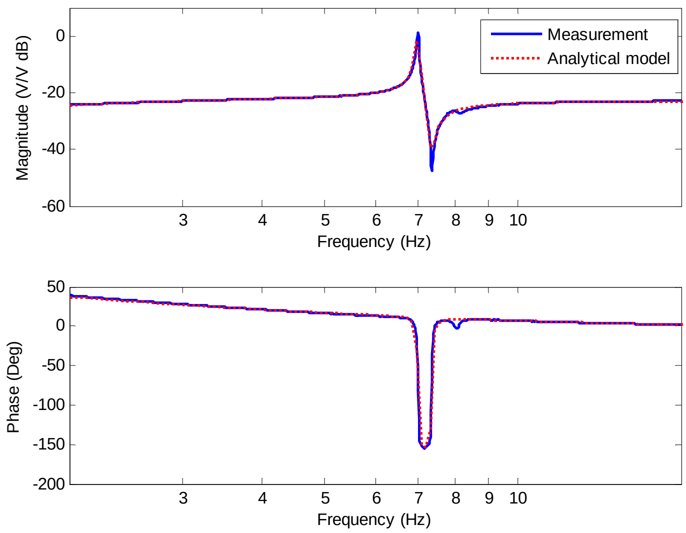

Figure 4: Experimentally measured and analytically estimated transfer function of the smart beam

4 LQG Controller Design

Linear-Quadratic-Gaussian (LQG) control is a modern state-space technique for designing optimal dynamic regulators. It enables one to trade off regulation performance and control effort, and allows including the measurement noise in the process. LQG design requires a state-space model of the plant and the state-space realization of the smart beam model in Equation 2 is of the form

$$\begin{aligned} \dot{x} &= Ax + B(u + w) \\ y &= Cx + D(u + w) + v \end{aligned} \tag{2}$$

The goal of the LQG regulator is to regulate the output value y around zero. The plant is driven by the process noise w and the control signal u, and the regulator relies on the noisy measurements $y_v=y+v$ to generate this control. In this study both w and v are modeled as white noise. Here, x is the state vector. A, B, C and D matrices are those obtained by the state space realization of the smart beam transfer function given in Equation 1. The matrices are given in Equation 3.

$$A=\begin{bmatrix} -0.1591 & 43.9598 & -0.4489 & 0.1183 & -0.3199 & 0.8792 \\ -43.9598 & -0.1087 & 0.3286 & -0.1098 & 0.2386 & -0.7390 \\ 0.4489 & 0.3286 & -4.4873 & 27.8862 & -3.4947 & 21.1486 \\ 0.1183 & 0.1098 & -27.8862 & -0.4370 & 34.0520 & -5.5300 \\ 0.3199 & 0.2386 & -3.4947 & -34.0520 & -2.7402 & 18.3420 \\ 0.8792 & 0.7390 & -21.1486 & -5.5300 & -18.3420 & -183.6586 \end{bmatrix},\quad B=\begin{bmatrix} -0.4384 \\ -0.3614 \\ 0.5802 \\ 0.1722 \\ 0.4176 \\ 1.2197 \end{bmatrix},$$
$$C=\begin{bmatrix} -0.4384 & 0.3614 & -0.5802 & 0.1722 & -0.4176 & 1.2197 \end{bmatrix},\quad D=\begin{bmatrix} 0.0645 \end{bmatrix} \tag{3}$$

The LQG regulator consists of an optimal state-feedback gain vector K and a Kalman state estimator. In LQG control, the regulation performance is measured by a quadratic performance criterion of the form

$$J(u)=\int_0^\infty \{x^T Qx + 2x^T Nu + u^T Ru\}dt \tag{4}$$

The weighting matrices Q, N and R are user specified and define the trade-off between regulation performance and control effort. In the design of LQG controller, one first seeks a state-feedback law u=-Kx that minimizes the cost function J(u). The minimizing gain matrix K is obtained by solving an algebraic Riccati equation. Finally, the design is completed by designing of the Kalman filter which is an optimal estimator when dealing with Gaussian white noise.

In this study, in order to synthesize a least possible order LQG controller, the smart beam model was reduced to a 2^{nd} order system. This was done by assuming that a 2^{nd} order system can characterize the first mode of the beam.

In Figure 5, block diagram of the developed LQG controller is given. A_r, B_r, C_r and D_r matrices are state space representation matrices of the reduced smart beam model $G_r(s)$. Degree of $G_r(s)$ is two. x^I is the estimated state vector by the Kalman filter.

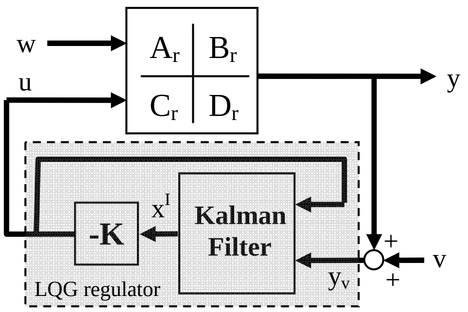

Figure 5: Block diagram of the developed LQG controller.

The frequency responses of the smart beam model G(s) and the reduced smart beam model $G_r(s)$ are given in Figure 6.

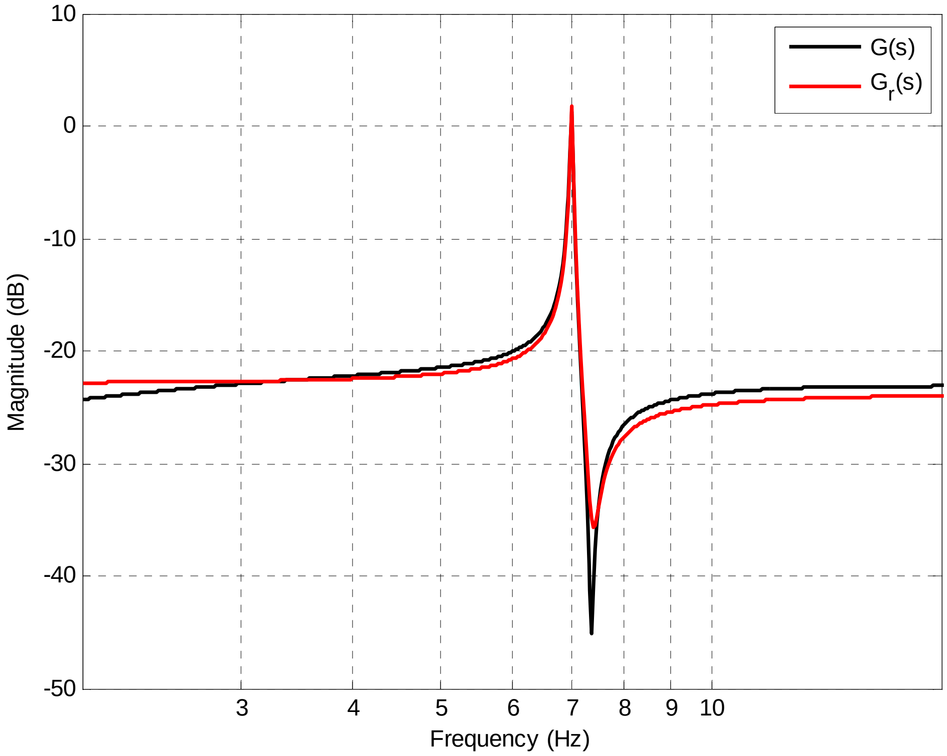

Figure 6: Frequency responses of the smart beam and the reduced smart beam model

5 Simulation Results of the Smart Beam

LQG control design was conducted for five different values of control effort weight R which limits the control signal u. Figure 7 shows the simulated closed loop frequency responses for different R values, together with the open loop frequency response. It can be seen that increasing R increases the effectiveness of the controller in the resonance region. In off-resonant regions increasing R decreases the effectiveness.

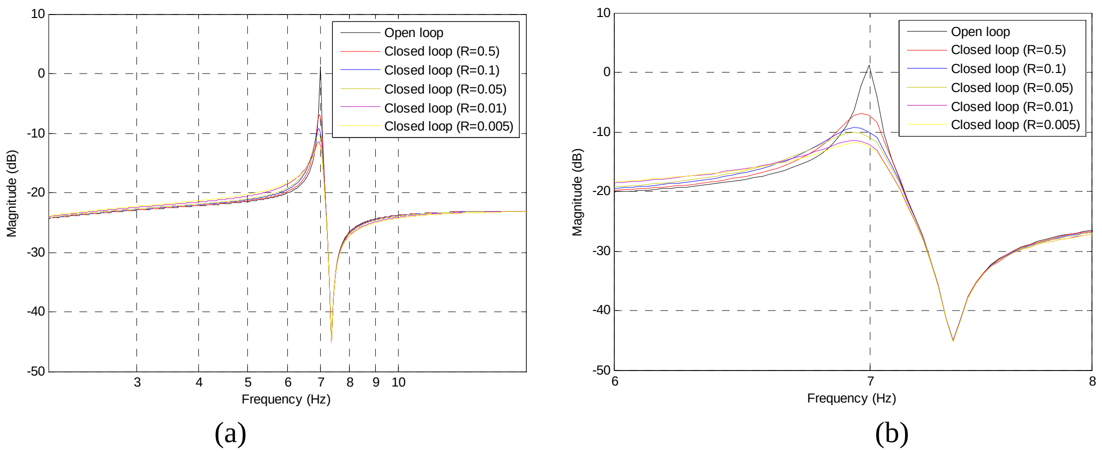

Figure 7: Simulated frequency response diagrams (a) Between 2 Hz – 18 Hz
(b) Zoomed around first resonance frequency

6 Experimental Results of the Smart Beam

The smart beam was given an initial 8 mm tip deflection and the ensuing motion was measured for open and closed loop time responses. The results are presented in Figure 8 and it shows the controlled time responses of the smart beam for R=0.5, R=0.1, R=0.05, R=0.01 and R=0.005 cases. The settling times were determined to be nearly 25, 15, 12, 4.5 and 4 seconds for decreasing R values in order. Hence, the designed controller for R=0.005 proves to be the most effective on suppressing the free vibrations of the smart beam.

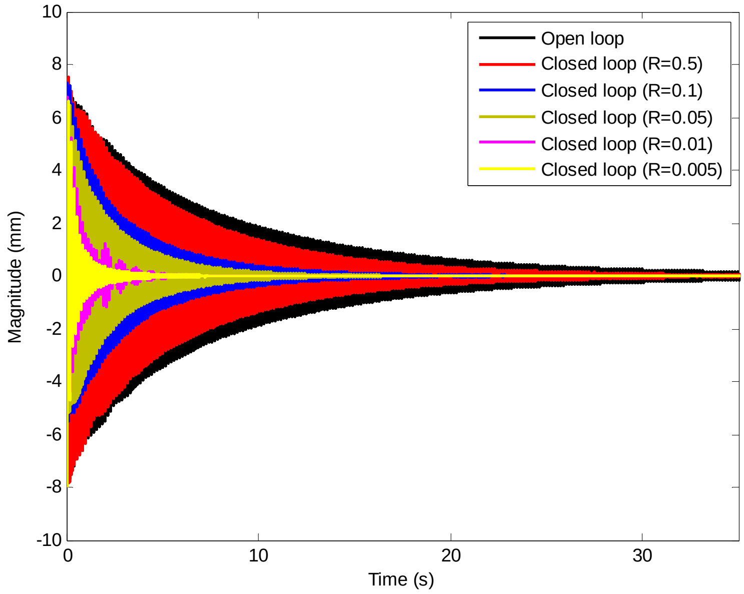

Figure 8: Free vibration response of the smart beam

Then, the smart beam was excited at its first resonance frequency (approximately at 7 Hz) by using the PZT patches as actuators. The effects of controllers on the suppression of the forced vibrations are shown in Figure 9. For these cases, the suppression rate, which is defined in Equation 5 at the first resonance frequency, were calculated approximately as 32, 51, 66, 82 and 87 percent, for R=0.5, R=0.1, R=0.05, R=0.01 and R=0.005 cases in order.

$$\text{Suppression Rate} = \frac{[\text{Open Loop Magnitude}]_{MAX} - [\text{Closed Loop Magnitude}]_{MAX}}{[\text{Open Loop Magnitude}]_{MAX}} \times 100 \qquad (5)$$

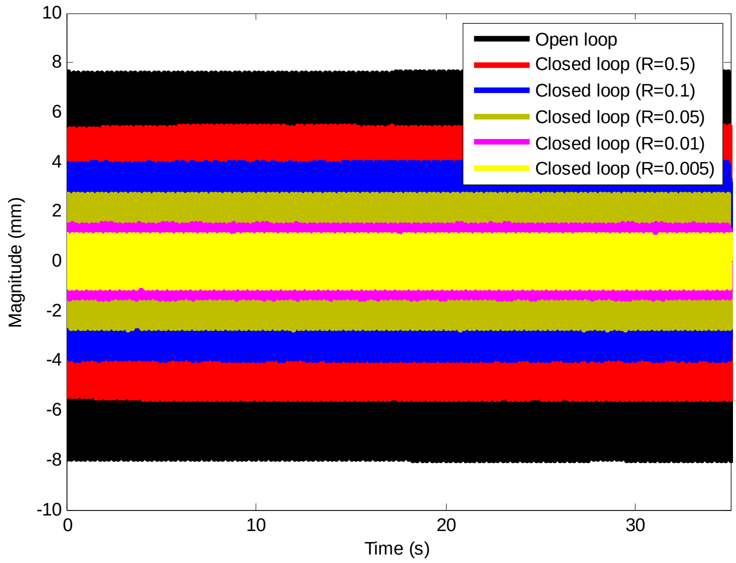

Figure 9: Forced vibration response of the smart beam at its first resonance frequency

The experimentally obtained open and closed loop frequency responses of the smart beam are given in Figure 10. It has been determined that the controllers with R=0.1 and R=0.05 have shifted the system resonance frequency to 6.875 Hz, R=0.01 controller to 6.625 Hz and R=0.005 controller to 6.5 Hz. In Figure 11, attenuation level, which is defined in Equation 6, of the control cases are demonstrated at the shifted frequency. It can be seen from Figures 10 and 11 that the decrease of the control effort value, R, has a tendency to shift the closed loop resonance frequency value to a lower frequency value. This is done despite an effective reduction at the open loop resonance level.

$$\text{Attenuation Level} = \left[\text{Open Loop Vibration Level}\right] - \left[\text{Closed Loop Vibration Level}\right] \tag{6}$$

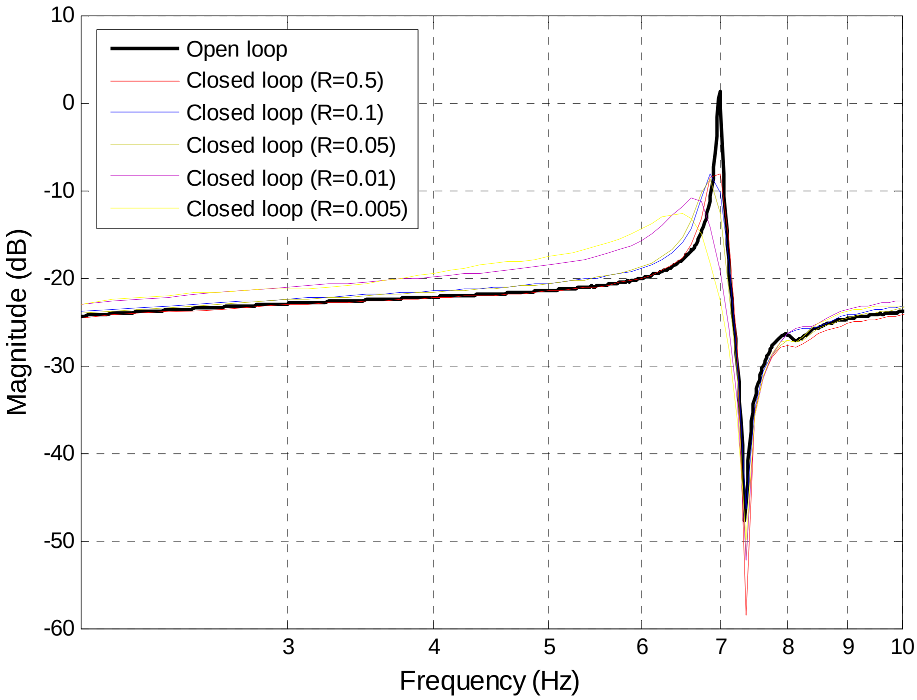

Figure 10: Open and closed loop frequency responses of the smart beam

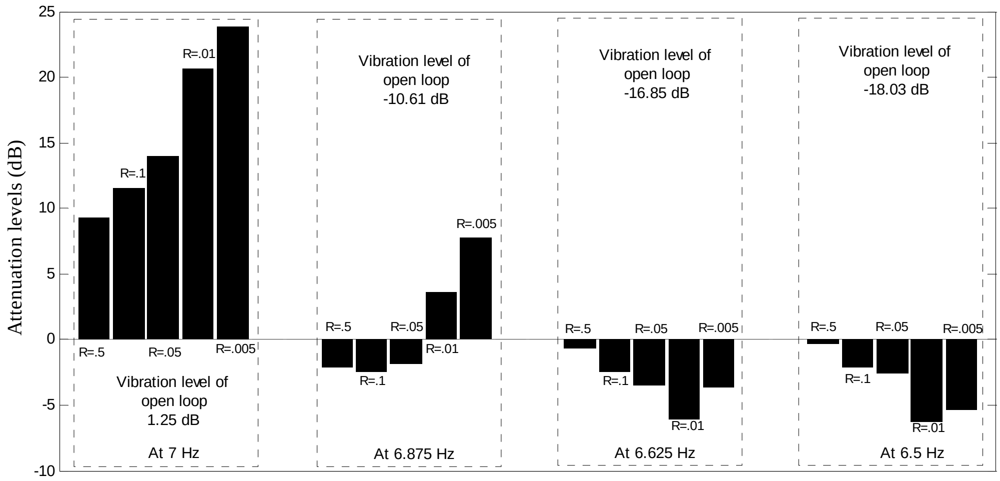

Figure 11: Attenuation levels at shifted resonance frequencies of the smart beam

7 Conclusion

In this paper, the system model of the smart beam was obtained by using experimental data. Then, the design and implementation of a second order LQG controller was presented for suppressing the first flexural vibrations of a smart beam. To design a controller with a low order is believed to be an important advantage especially for commercial applications.

The design was fulfilled for five different values of the control effort. Increase in the control effort value provided an improvement in the free response and forced response of the smart beam. However this caused a shift in the resonance frequency and resulted in performance loss at low frequency off-resonant region.

References

1. Caliskan T (2002). *Smart Materials and Their Applications in Aerospace Structures*. PhD Thesis, Middle East Technical University.
2. Sahin M Karadal F M Yaman Y Kircali O F Nalbantoglu V Ulker F D Caliskan T (2008). Smart Structures and Their Applications on Active Vibration Control: Studies in the Department of Aerospace Engineering, METU. *J. Electroceramics*, 20(3-4), 167–174.
3. Ulker D F (2003). *Active Vibration Control of Smart Structures*. Master Thesis, Middle East Technical University.
4. Kircali O F Yaman Y Nalbantoglu V Sahin M Karadal F M Ulker F D (2008). Spatial Control of a Smart Beam. *J. Electroceram*, 20, 175–185.
5. Aridogan U (2010). *Performance Evaluation of Piezoelectric Sensor/Actuator on Investigation of Vibration Characteristics and Active Vibration Control of a Smart Beam*, Master Thesis, Middle East Technical University.
6. Sensor Technologies Limited (2002). BM-500 Lead Zirconate Titanate Product Data Sheet.
7. Balas G J Doyle J C Glover K Packard A Smith R (2001). *μ Analysis and Synthesis Toolbox For Use with MATLAB.*